Available online at www.sciencedirect.com
ScienceDirect
Polymer 48 (2007) 1329–1342
polymer
www.elsevier.com/locate/polymer

Complicated phase behavior and ionic conductivities of PVP-*co*-PMMA-based polymer electrolytes

Chun-Yi Chiu, Ying-Jie Yen, Shiao-Wei Kuo, Hsien-Wei Chen, Feng-Chih Chang*

Institute of Applied Chemistry, National Chiao-Tung University, Hsin-Chu 30043, Taiwan

Received 15 June 2006; received in revised form 13 December 2006; accepted 28 December 2006
Available online 12 January 2007

Abstract

We have used DSC, FTIR spectroscopy, and ac impedance techniques to investigate the interactions that occur within complexes of poly(vinylpyrrolidone-*co*-methyl methacrylate) (PVP-*co*-PMMA) and lithium perchlorate ($LiClO_4$) as well as these systems' phase behavior and ionic conductivities. The presence of MMA moieties in the PVP-*co*-PMMA random copolymer has an inert diluent effect that reduces the degree of self-association of the PVP molecules and causes a negative deviation in the glass transition temperature (T_g). In the binary $LiClO_4$/PVP blends, the presence of a small amount of $LiClO_4$ reduces the strong dipole–dipole interactions within PVP and leads to a lower T_g. Further addition of $LiClO_4$ increases T_g as a result of ion–dipole interactions between $LiClO_4$ and PVP. In $LiClO_4$/PVP-*co*-PMMA blend systems, for which the three individual systems—the PVP-*co*-PMMA copolymer and the $LiClO_4$/PVP and $LiClO_4$/PMMA blends—are miscible at all compositional ratios, a phase-separated loop exists at certain compositions due to a complicated series of interactions among the $LiClO_4$, PVP and PMMA units. The PMMA-rich component in the PVP-*co*-PMMA copolymer tends to be excluded, and this phenomenon results in phase separation. At a $LiClO_4$ content of 20 wt% salt, the maximum ionic conductivity occurred for a $LiClO_4$/VP57 blend (i.e., 57 mol% VP units in the PVP-*co*-PMMA copolymer).

Keywords: Polymer electrolyte; Ionic conductivity; Phase behavior

1. Introduction

Polymer electrolytes are compounds formed through the dissolution of salts into polar and high-molecular weight macromolecules that can interact strongly with cations. The proposed use of solvent-free polymer electrolytes for high-energy density batteries and other solid-state electrochemical devices [1–5] has spurred considerable interest in the ion-transport properties of these materials. For most potential applications, it is desirable that the solid polymer electrolytes display a reasonable conductivity (ca. 10^{-4} S cm^{-1}), dimensional stability, processability, and flexibility under ambient conditions. Great progress has been made over the last 20 years in increasing the level of ionic conductivity that polymer electrolytes exhibit [6]. In recent years, however, the levels of ionic conductivity have been limited to a ceiling of ca. 10^{-4} S cm^{-1} at room temperature, despite innovations in the design of flexible polymers and the use of salts containing asymmetric anions capable of suppressing crystallinity. Unfortunately, such levels of ionic conductivity are insufficient for many lithium battery applications [7,8]. It seems necessary for us to change our way of thinking concerning how to optimize and further increase the ionic conductivity. We must determine the fundamental interactions within polymer electrolytes if we are to better understand the ion-transport mechanism and, hence, improve their performance.

Poly(vinylpyrrolidone) (PVP) is amorphous and exhibits a high value of T_g because of the presence of its rigid pyrrolidone groups. PVP's tertiary amide carbonyl groups possess marked Lewis base character such that they form a variety

* Corresponding author. Tel./fax: +886 3 5131512.
E-mail address: changfc@mail.nctu.edu.tw (F.-C. Chang).

0032-3861/$ - see front matter © 2007 Elsevier Ltd. All rights reserved.
doi:10.1016/j.polymer.2006.12.059

of complexes with a range of inorganic salts [9]. Unfortunately, the high T_g feature of Li–PVP polymer electrolytes tends to limit the mobility of the ions and results in poor ionic conductivity.

On the other hand, gel-type polymer electrolytes based on poly(methyl methacrylate) (PMMA) [10,11] have been proposed for use in lithium batteries mainly because of their beneficial effects on the stabilization of the lithium–electrode interface [12]. The reasonable conductivity achieved by such plasticizer films is, however, offset by PMMA's relatively poor mechanical properties at a high concentration of the plasticizer. Furthermore, the interactions between Li^+ cations and PMMA are significantly weaker than those of other polymer matrixes, such as poly(ethylene oxide) and PVP; therefore, PMMA is less able to dissociate the lithium salt, which further weakens its cation transporting function. The Li–PMMA polymer electrolyte in its all-solid state also exhibits a low ionic conductivity.

Because PVP and PMMA possess complementary advantages for their use as polymer electrolytes, we became interested in studying polymer electrolytes formed by incorporating lithium perchlorate into mixtures of PVP and PMMA. Here, we chose to use a PVP-*co*-PMMA random copolymer, synthesized through free radical polymerization, as a replacement since the random copolymer has higher miscibility behavior than that of blend system. It seemed reasonable to expect that a gel-type polymer electrolyte based on PVP-*co*-PMMA may not only sustain the mechanical properties of a PMMA-based gel polymer electrolyte but also increase the dissolution of the lithium salt because of the strong polarity of the PVP units [9]. To the best of our knowledge, no previous studies have been reported describing the influences that the miscibility behavior and the interaction mechanism have on the ionic conductivity in polymer electrolytes comprising $LiClO_4$ and random copolymers. In this study, we employed differential scanning calorimetry (DSC), Fourier transform infrared (FTIR) spectroscopy, and alternating current (ac) impedance techniques to investigate the interactions within and related conductivities of all solid-state polymer electrolytes formed from $LiClO_4$/PVP-*co*-PMMA blend systems.

2. Experimental

2.1. Materials

Benzene, pyridine, azobisisobutyronitrile (AIBN), *N*-vinyl-2-pyrrolidone (VP), methyl methacrylate (MMA), and lithium perchlorate ($LiClO_4$) were purchased from Aldrich Chemical Co. AIBN was purified through recrystallization from ethanol. Benzene and pyridine were fractionally distilled over CaH_2. The monomers MMA and VP were purified through vacuum distillation over CaH_2, the fractions were collected at room temperature and 50 °C, respectively. $LiClO_4$ was dried in a vacuum oven at 80 °C for 24 h and stored in a desiccator prior to use.

2.2. Synthesis of poly(N-vinyl-2-pyrrolidone-co-methyl methacrylate) (PVP-co-PMMA) copolymers

Solution copolymerization of *N*-vinyl-2-pyrrolidone with methyl methacrylate was performed in benzene at 80 °C under a nitrogen atmosphere in a glass reaction flask equipped with a condenser (Scheme 1). AIBN (3 wt% with respect to monomers) was employed as an initiator for free radical polymerization. To determine the reactivity ratio, the sample of the copolymer was taken from the reaction flask during the early stages of copolymerization when the degree of conversion was low (between 4 and 9%) [13]. The mixture was stirred for ca. 24 h and then poured into excess ethyl ether with vigorous agitation to precipitate and purify the product. The filtered polymer product was dried until it reached a constant weight.

2.3. Characterization

The molecular weights and polydispersities of the synthesized copolymers were determined through gel permeation chromatography (GPC) at 50 °C using *N*,*N*-dimethylformamide (DMF) as the eluent and polystyrene standards for calibration of the molecular weight. The composition of the copolymer was further ascertained by means of ^{1}H NMR spectroscopy and elementary analysis (EA).

The ^{1}H NMR spectrum of the copolymer was recorded in deuterated chloroform ($CDCl_3$) solution at 25 °C using a Varian UNITY INOVA-400 NMR spectrometer. EA was performed in an oxidative atmosphere at 1021 °C using a Heraeus CHN-O Rapid Elementary Analyzer. The copolymer compositions of VP and MMA correspond to repeating units of C_6H_9NO and $C_5H_8O_2$, respectively. The VP content (mol%) was determined using Eq. (1); it is based on the content of C and N atoms [14].

$$\mathrm{VP(mol\%)} = \frac{30\mathrm{N}}{7\mathrm{C} - 6\mathrm{N}} \times 100 \tag{1}$$

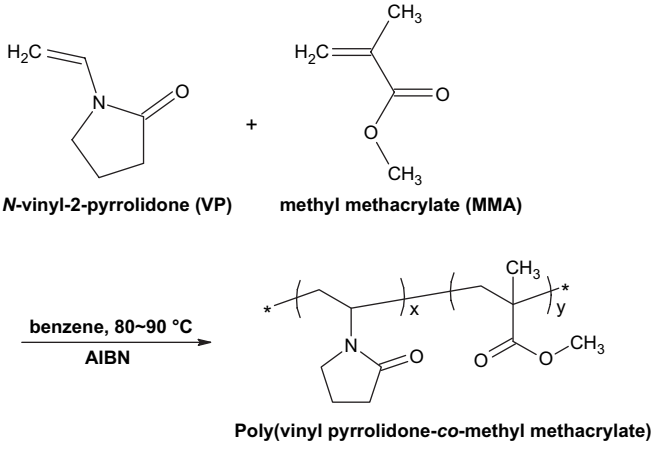

Scheme 1. Synthesis of PVP-*co*-PMMA random copolymer.

2.4. Sample preparation

$LiClO_4$/PVP-*co*-PMMA polymer electrolytes in various blend compositions were prepared through solution casting. The desired amounts of PVP-*co*-PMMA and $LiClO_4$ were dissolved in pyridine and stirred continuously for 24 h at 60 °C. The solution was cast onto a Teflon dish and maintained at 50 °C for an additional 24 h to remove the solvent; the sample was then dried under vacuum at 80 °C for two days. To prevent its contact with air or moisture, the polymer electrolyte film was transferred into a glove box under a nitrogen atmosphere.

2.5. Differential scanning calorimetry (DSC)

Thermal analyses were performed using a DSC instrument (DuPont TA 2010). The instrument was calibrated with indium standards and the analyses were conducted under a nitrogen flow rate of ca. 40 mL/min. The sample was heated sequentially from 30 to 200 °C for the first scan, maintained at 200 °C for 10 min, cooled rapidly to 0 °C, and then reheated to 300 °C. The glass transition temperature (T_g) was obtained as the inflection point of the heat capacity jump recorded at a scan rate of 20 °C/min.

2.6. Fourier transform infrared (FTIR) spectroscopy

Infrared spectra of the polymer films were recorded at 120 °C using a conventional KBr disk method. All polymer films were prepared under a N_2 atmosphere. The pyridine solution was cast onto a KBr disk, from which the solvent was evaporated under vacuum at 80 °C for 48 h. All films used in this study were sufficiently thin to obey the Beer–Lambert law. FTIR spectra were recorded over the range 4000–400 cm^{-1} using a Nicolet AVATAR 320 FTIR spectrophotometer (Nicolet Instruments, Madison, WI); 32 scans were collected at a spectral resolution of 1 cm^{-1}.

2.7. Conductivity measurements

The frequency-dependent impedance properties (from 10 to 10 Hz) of the polymer complexes were measured using an Autolab designed by Eco Chemie. For conductivity measurements, the sample was pressed into disks having thicknesses varying from 0.50 to 0.15 mm. The disks were loaded into a sealed conductivity cell between stainless-steel blocking electrodes and the impedance responses were measured at temperatures from 30 to 100 °C.

3. Results and discussion

3.1. PVP-co-PMMA copolymer characterization

Copolymerization of *N*-vinyl-2-pyrrolidone with methyl methacrylate was performed at 80 °C using AIBN as the initiator (Scheme 1). A series of copolymers were prepared at various VP and MMA monomer concentrations. The VP content (mol%) in the copolymer was determined through ^1H NMR spectroscopy and EA; Table 1 summarizes the results. Because traces of water present in PVP-*co*-PMMA copolymers may have led to overestimation of the integration of the PVP signals in the ^1H NMR spectra, which would result in (false) slightly higher PVP readings in the products than in the feeds, for greater accuracy it was necessary to perform EA. The abundances of N and C atoms determined from EA were applied to calculate the VP content using Eq. (1), i.e., because of the presence of moisture, the H atom content of the polymers was not taken into account in calculating the VP content. From a comparison of the results obtained from the EA and ^1H NMR spectroscopic data, the EA results were quite reproducible, regardless of the presence of moisture. Indeed, the VP contents determined from the ^1H NMR spectra were usually 5–10% greater than those determined through EA. Thus, EA was a more suitable technique for quantification of the VP content in the PVP-*co*-PMMA copolymers and, therefore, in

Table 1
PVP-*co*-PMMA copolymer compositional and molecular-weight data[a]

Polymer[b]	Monomer feed (mol%)		Polymer composition (mol%)				M_n[e] (g/mol)	M_w/M_n[e]	T_g[f] (°C)
			EA[c]		NMR[d]				
	VP	MMA	VP	MMA	VP	MMA			
PVP	100	0	100	0	100	0	18 200	2.33	181
VP79	78.3	21.7	78.8	21.2	80.8	19.2	18 700	2.40	161
VP57	57.5	42.5	57.0	43.0	62.6	37.4	23 000	2.23	144
VP47	47.4	52.6	46.8	53.2	52.9	47.1	17 000	2.29	139
VP39	37.5	62.5	38.5	61.5	40.7	59.3	20 300	2.52	134
VP19	18.4	81.6	19.4	80.6	18.7	81.3	22 100	2.00	123
PMMA	0	100	0	100	0	100	25 700	1.76	121

[a] Polymerization conditions: initiator = AIBN; solvent = benzene; temperature = 80 °C.
[b] Labeling based on VP content in the PVP-*co*-PMMA copolymers obtained from EA.
[c] Calculated from the elementary analyzer using Eq. (1).
[d] Obtained form the ^1H NMR spectra.
[e] M_n: number-average molecular weight, M_w: weight-average molecular weight, and M_w/M_n were all determined by GPC using polystyrene standards and DMF as the eluent.
[f] Characterized by DSC thermograms.

the following discussion the sample codes for these copolymers are based on the VP contents obtained through EA.

Table 1 lists the monomer feed ratios and resultant copolymer compositions from which we calculated the reactivity ratios (r_1 and r_2) using the methodology of Kelen and Tüdös [15–17]. All polymerizations were performed in benzene, under the conditions described inSection 2, and terminated at monomer conversions below 10% to minimize any errors due to changes in the feed ratios. The values of r_1 and r_2 represent the ratios of the homo- and cross-propagation rate constants for each monomer (i.e., $r_1 = k_{11}/k_{12}$ and $r_2 = k_{22}/k_{21}$, where k is the rate constant). The Kelen–Tüdös equation is given by Eq. (2):

$$\eta = \left(r_1 + \frac{r_2}{\alpha}\right)\xi - \frac{r_2}{\alpha} \tag{2}$$

where

$$\eta = \frac{G}{\alpha + F} \text{ and } \xi = \frac{F}{\alpha + F}$$

The values of F and G can be obtained from the quantities x and y, where x is the ratio of molar concentration of monomers 1 and 2 (M_1/M_2) and y is the mole ratio of these monomers in the copolymer (dM_1/dM_2); namely, $F = x^2/y$ and $G = x(y-1)/y$. The value of α is defined by the expression $\alpha = (F_m F_M)^{1/2}$, where F_m and F_M are the lowest and highest values of F obtained from the experimental data. By plotting the values of η versus ξ, we obtain the values of r_2 and r_1 from the intercept and slope. Fig. 1 displays the results from which we calculated the values of r_{PVP} and r_{PMMA} as 0.97 and 0.94, respectively. In a previous paper [18], it was proposed that copolymerization behavior be termed "ideal" when the product of the two reactivity ratios is unity (i.e., $r_1 r_2 = 1$). Moreover, when $r_1 = r_2 = 1$, the two monomers display equal reactivities toward both propagating species. In this case, the copolymer composition is the same as the comonomer feed with a random distribution of these two monomers along the copolymer chain; such behavior is referred to as random or Bernoullian growth.

In this study, our PVP-*co*-PMMA copolymers were synthesized through free radical polymerization in essentially a random manner, with a slight tendency toward the formation of an ideal copolymer ($r_{PVP} \times r_{PMMA} = 0.91$).

Table 1 lists the values of T_g of our samples. Several empirical and semi-empirical equations have been suggested for predicting the dependence of T_g on the copolymer composition. In this study, we believed that the most suitable equation for a weakly interacting system would be the Gordon–Taylor equation [19,20]:

$$T_g = \frac{w_1 T_{g1} + k w_2 T_{g2}}{w_1 + k w_2} \tag{3}$$

where w_1 and w_2 are the weight fractions of the components, T_{g1} and T_{g2} represent the corresponding glass transition temperatures, and k is the fitting constant. Fig. 2 displays plots of T_g versus the PVP weight fractions of the PVP-*co*-PMMA copolymers. We obtained a value of k of 0.45 through a nonlinear least-squares "best fit" analysis. This low value of k implies that weak interactions exist between the VP and MMA units in these copolymers [21]. The even distribution of MMA moieties means that these units play the role of an inert diluent to hinder the self-association of the PVP moieties. Moreover, at a low PVP content (20 mol%), the diluent plays the dominant role and results in a relatively lower value of T_g. In contrast, dipole–dipole interactions between the PVP units are dominant at higher PVP content; they result in higher values of T_g. The Fox and Gordon–Taylor equations are generally recognized to hold true for miscible blends or copolymers in which only weak intermolecular interactions exist. We found it very useful to employ these equations to analyze the compositional behavior of our PVP-*co*-PMMA copolymers. The negative deviation from the Fox equation that we observed in this study suggests that one of the components in this PVP-*co*-PMMA random copolymer system possessed a stronger self-association (e.g., to form dimers or multimers) than did the other [22,23]. As a result, the values of T_g for the PVP-*co*-PMMA samples having higher PVP contents displayed

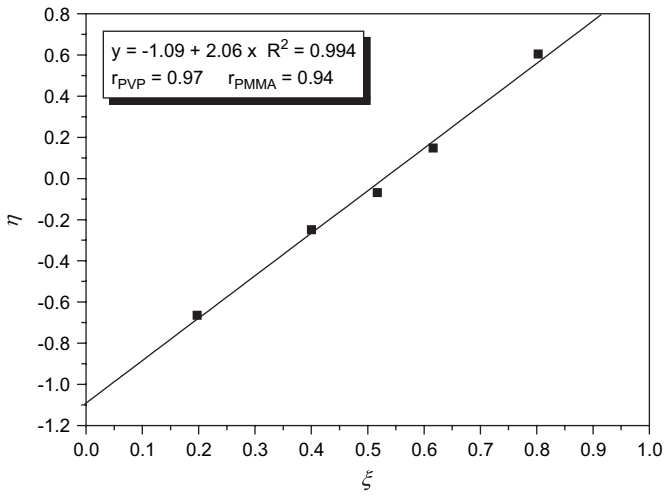

Fig. 1. Kelen–Tüdös plot for PVP-*co*-PMMA copolymers.

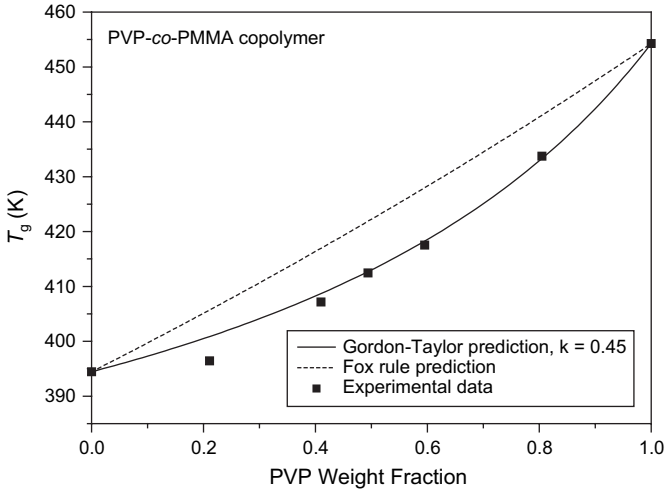

Fig. 2. Plot of T_g versus the PVP content of the PVP-*co*-PMMA copolymers.

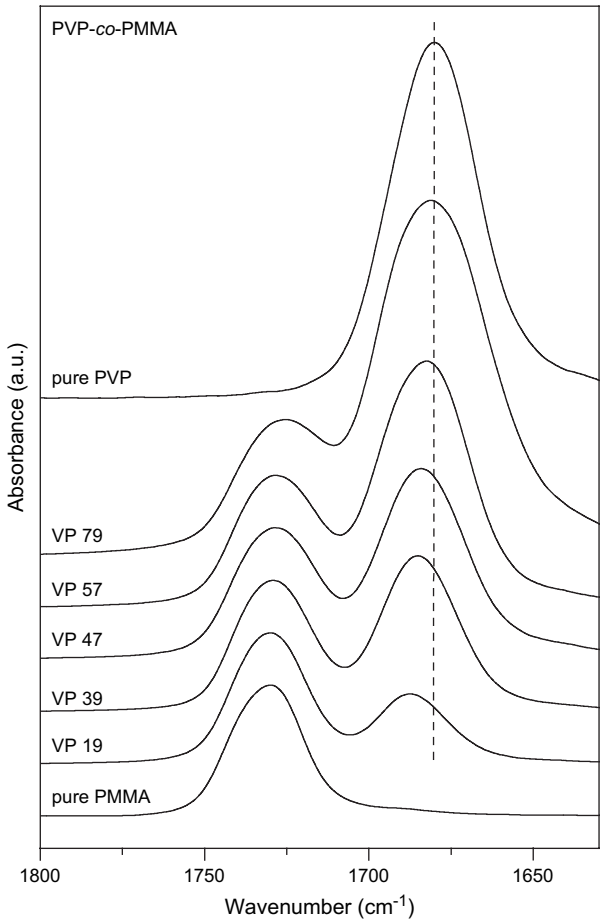

Fig. 3. IR spectra (1800–1630 cm^{-1}), recorded at 120 °C, of neat PVP, neat PMMA, and a series of PVP-*co*-PMMA copolymers containing various PVP contents.

relatively smaller deviations from either of the equations than did those having lower PVP contents [21,24,25].

Fig. 3 displays scale-expanded infrared spectra, recorded at 120 °C and plotted in the range 1800–1630 cm^{-1}, for neat PVP, neat PMMA, and a series of PVP-*co*-PMMA copolymers. The absorption peaks at ca. 1680 and 1730 cm^{-1} are assigned to the carbonyl vibration bands of PVP and PMMA, respectively. Interestingly, we found that the maximum of the carbonyl vibration band of PVP shifted slightly toward higher frequency when the MMA moiety was incorporated into the PVP. This finding implies that the strength of the dipole–dipole interactions of the PVP units was reduced, or that they were eliminated completely, as a result of the MMA moieties acting as inert diluents [26]. Therefore, the behavior observed in the IR spectra is consistent with the DSC results (Fig. 2), i.e., the diluent effect is responsible for the observed decrease in the values of T_g of the PVP-*co*-PMMA copolymers.

3.2. $LiClO_4$/PVP and $LiClO_4$/PMMA binary blends

It has been reported that the properties of polymer/salt mixtures can change dramatically as a result of ionic aggregation [27–29]. We performed thermal analyses first to determine whether the properties of $LiClO_4$/PVP and $LiClO_4$/PMMA blends were affected by the addition of lithium perchlorate. Fig. 4 displays DSC thermographs of $LiClO_4$/PMMA and $LiClO_4$/PVP blends containing various $LiClO_4$ salt contents. Fig. 4a indicates that the maximum T_g increment was ca. 145 °C for PMMA containing 20 wt% $LiClO_4$. Ionic interactions or ionic cluster formation in the amorphous region of the ionomer usually resembles physical cross-linking. The mobility of a polymer chain is restrained through such physical cross-linking and, thus, it leads to higher glass transition temperatures relative to those of the mother polymer. Generally, the value of T_g increases gradually upon the addition of the salt because of the increased number of ion–polymer and ion–ion interactions; a maximum glass transition temperature is usually achieved at a certain content of $LiClO_4$. Excess $LiClO_4$ tends to self-aggregate, which causes the value of T_g of $LiClO_4$/PMMA blends to decrease through a dilution effect [30,31]. It has been demonstrated quite clearly that most polymer/salt blends—such as those involving poly(ethylene oxide) (PEO)/lithium [32], poly(2-ethyl-2-oxazoline) (PEtOx)/silver [33], and poly(4-vinylpyridine) (P4VP)/zinc [28]—exhibit similar trends as those DSC phenomena described above.

The $LiClO_4$/PVP blend, however, presents (Fig. 4b) a novel behavior for its variation in glass transition temperature upon increasing the $LiClO_4$ salt. The addition of a low amount of $LiClO_4$ (5 wt%) actually causes a decrease in the value of T_g of PVP. This phenomenon is unusual when compared with the results obtained previously for other polymer/salt blends. Relative to PMMA, PVP is a more water-soluble polymer because the tertiary amide carbonyl groups exhibit stronger Lewis basic character (dipole moment: ca. 4 D) [34,35]. Therefore, it seems reasonable to expect that PVP possesses a higher value of T_g (181 °C) primarily because of its strong intermolecular dipole–dipole interactions, even though other factors may also contribute. The presence of $LiClO_4$ at a relative low concentration reduces the degree of self-association of the PVP units and results in lower values of T_g [25] because the electron donor groups of PVP interact, through ion–dipole interaction, with the electron acceptor species (i.e., the Li^+ cations). As a result, two competitive interactions exist: self-association of PVP through dipole–dipole interactions and ion–dipole interactions between Li^+ cations and the carbonyl groups of PVP. Although the mobility of a polymer chain tends to be restrained upon the addition of $LiClO_4$, which results in higher values of T_g, for PVP this effect is offset by the reduction in the strength of the dipole–dipole interaction units, which results in the lower values of T_g at low $LiClO_4$ concentrations. As indicated in Fig. 4b, when the $LiClO_4$ content increased from 0 to 30 wt%, the value of T_g increased from 181 to 191 °C. This temperature increment ($\Delta T_g =$ 10 °C) is less than those that we observed previously for $LiClO_4$/PEO ($\Delta T_g =$ ca. 35 °C) and $ZnClO_4$/P4VP ($\Delta T_g =$ ca. 140 °C) blend systems [28,32]. Further addition of $LiClO_4$ to the $LiClO_4$/PVP blend system (from 30 to 40 wt%) led to the value of T_g increasing dramatically up to its maximum at 233 °C. When we increased the $LiClO_4$ content to 50 wt%, however, the value of T_g decreased. According to these

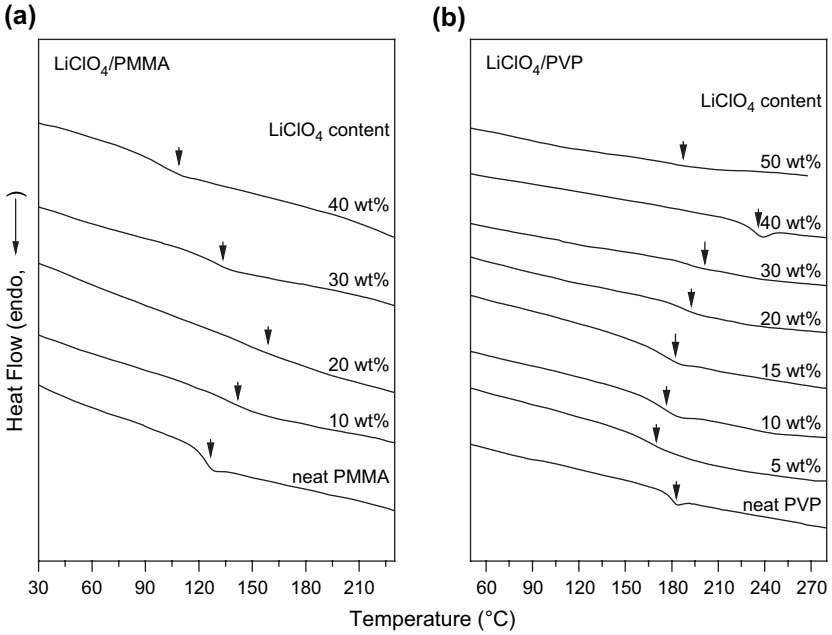

Fig. 4. DSC scans of (a) $LiClO_4$/PVP and (b) $LiClO_4$/PMMA blends of varying compositions.

observations, the optimal ion–dipole interaction (strongest enhancement of T_g) occurred at a $LiClO_4$-to-PVP ratio of 40/60. An excess $LiClO_4$ content (>40 wt%) resulted in salt aggregation and, thus, a lower value of T_g, because of an increasing interchain distance at concentrations above the optimized lithium salt content [33].

We performed FTIR spectroscopic characterizations to further understand the mechanism through which the variations in T_g occur for the $LiClO_4$/PMMA and $LiClO_4$/PVP blend systems. Monitoring of the carbonyl stretching bands as a function of the blend composition is the method employed most frequently for quantifying the relative fractions of free and bonded carbonyl sites within PMMA or PVP polymer chains. Fig. 5 presents the carbonyl stretching absorptions, ranging from 1800 to 1550 cm^{-1}, in the IR spectra recorded at 120 °C of $LiClO_4$/PVP blends containing various $LiClO_4$ contents. The stretching band of the "free" carbonyl groups of uncomplexed PVP appears at 1680 cm^{-1}; this band is asymmetric and significantly broader than those of other noncomplexed carbonyl units [35–37]. For example, Painter and co-workers [38,39] demonstrated that the real "free" or "unperturbed" carbonyl stretching band of the model compound ethyl pyrrolidone (EPr) occurs at ca. 1708 cm^{-1}. The carbonyl stretching band of PVP obviously broadens and shifts to a lower frequency (ca. 1680 cm^{-1}) because of the strong self-association of PVP molecules (i.e., through dipole–dipole interactions between its pyrrolidone groups). Thus, there are very few truly "free" carbonyl units in the PVP; the carbonyl band observed in the FTIR spectrum of PVP actually consists of bands from a large number of associated species (multimers).

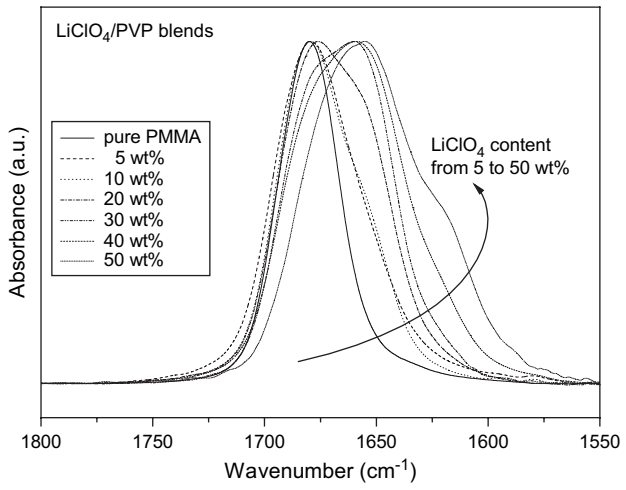

Fig. 5. IR spectra (C=O stretching region), recorded at 120 °C, of $LiClO_4$/PVP blends containing varying $LiClO_4$ contents.

As the $LiClO_4$ content increased, the carbonyl bands in Fig. 5 broaden gradually, and a new band appears at ca. 1654 cm^{-1} as a result of coordination between the Li^+ cation and the oxygen atom on the carbonyl group of PVP. A distinct third band appears at an even lower frequency (ca. 1630 cm^{-1}) when the $LiClO_4$ content is above 20 wt%. The lower frequency of this band suggests that an even stronger interaction occurs involving the carbonyl groups of PVP. In addition, its relative intensity increases upon increasing the $LiClO_4$ content. Thus, we believe that the carbonyl absorption band at ca. 1630 cm^{-1} corresponds to the carbonyl groups of PPV that interact simultaneously with several Li^+ cations. To further elucidate the effect that the $LiClO_4$ content has on the charge environment surrounding the carbonyl groups of PVP, in Fig. 6 we display the relative fractions of "uncomplexed" and "complexed" C=O sites obtained through decomposing C=O stretching band into two or three Gaussian peaks [38,40]; Table 2 summarizes the results. We assign

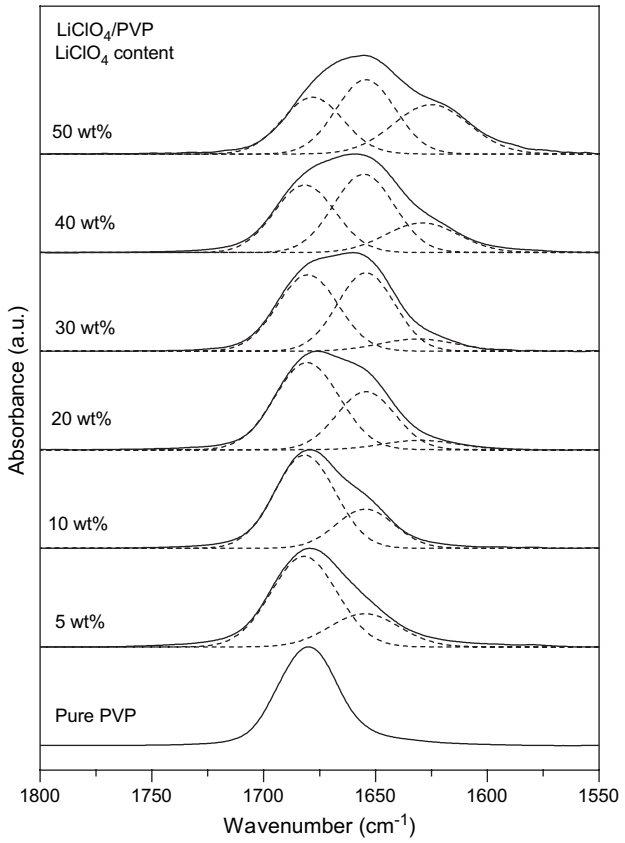

Fig. 6. Deconvolution of IR spectra (carbonyl stretching region: 1800–1550 cm^{-1}), recorded at 120 °C, of $LiClO_4$/PVP blends containing various $LiClO_4$ contents.

the carbonyl stretching bands located at 1680, 1654, and 1630 cm^{-1} to the ''uncomplexed,'' ''complexed I,'' and ''complexed II'' C=O units, respectively. The relative intensity of the ''uncomplexed'' C=O band decreased upon increasing the $LiClO_4$ content. Moreover, the initial addition of 5 wt% $LiClO_4$ caused the peak position of the ''uncomplexed'' C=O band to shift slightly to higher frequency (from 1680 to 1682 cm^{-1}), presumably because of a reduction in the number of dipole–dipole interactions between the PVP

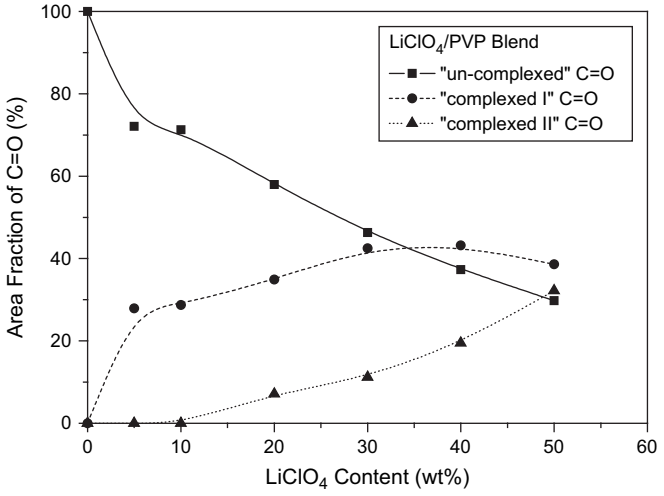

Fig. 7. Effect that the $LiClO_4$ concentration has on the signals of the ''free'' and ''complexed'' C=O bands.

units. Fig. 7 provides a summary of the fractional area versus the $LiClO_4$ content for the ''uncomplexed'' and two ''complexed'' C=O bands. The relative fractions of both the ''complexed I'' and the ''complexed II'' C=O bands increased upon increasing the $LiClO_4$ content up to 40 wt%, but after that the relative fraction of the ''complexed I'' C=O band began to decrease while that of the ''complexed II'' C=O band continued to increase. That is to say, complex I transformed gradually into complex II when the concentration of $LiClO_4$ increased. This finding provides evidence that the formation of complex II is more favorable at higher concentrations of $LiClO_4$. Furthermore, it is evident that not all of the added Li^+ cations associate with the carbonyl groups to form polymer–salt complexes: some ''uncomplexed'' C=O groups remain even at excessively high $LiClO_4$ concentrations. This result indicates that the Li^+ cations in the blend are in the equilibrium state which is between binding to their ClO_4^- counterion and to the C=O groups. Accordingly, these results are consistent with the phenomenon we observed from the DSC analyses.

Table 2
Curve-fitting results of infrared spectra of C=O group stretching region recorded at 120 °C for the $LiClO_4$/PVP and $LiClO_4$/PMMA blends with various $LiClO_4$ salt contents

Polymer	$LiClO_4$, wt%	Free C=O			Primary complexed C=O			Secondary complexed C=O		
		ν, cm^{-1}	$w_{1/2}$, cm^{-1}	A_f, %	ν, cm^{-1}	$w_{1/2}$, cm^{-1}	A_f, %	ν, cm^{-1}	$w_{1/2}$, cm^{-1}	A_f, %
PVP	0	1680	33	100						
	5	1682	34	72	1655	33	28			
	10	1681	32	71	1655	31	29			
	20	1681	34	58	1654	31	35	1630	39	7
	30	1680	32	46	1654	31	43	1631	40	11
	40	1681	32	37	1654	32	43	1632	39	20
	50	1678	32	30	1654	31	38	1625	40	32
PMMA	0	1731	22	100						
	10	1730	22	81	1706	31	19			
	20	1730	21	68	1705	32	32			
	30	1730	21	63	1705	32	37			
	40	1729	22	60	1704	32	40			

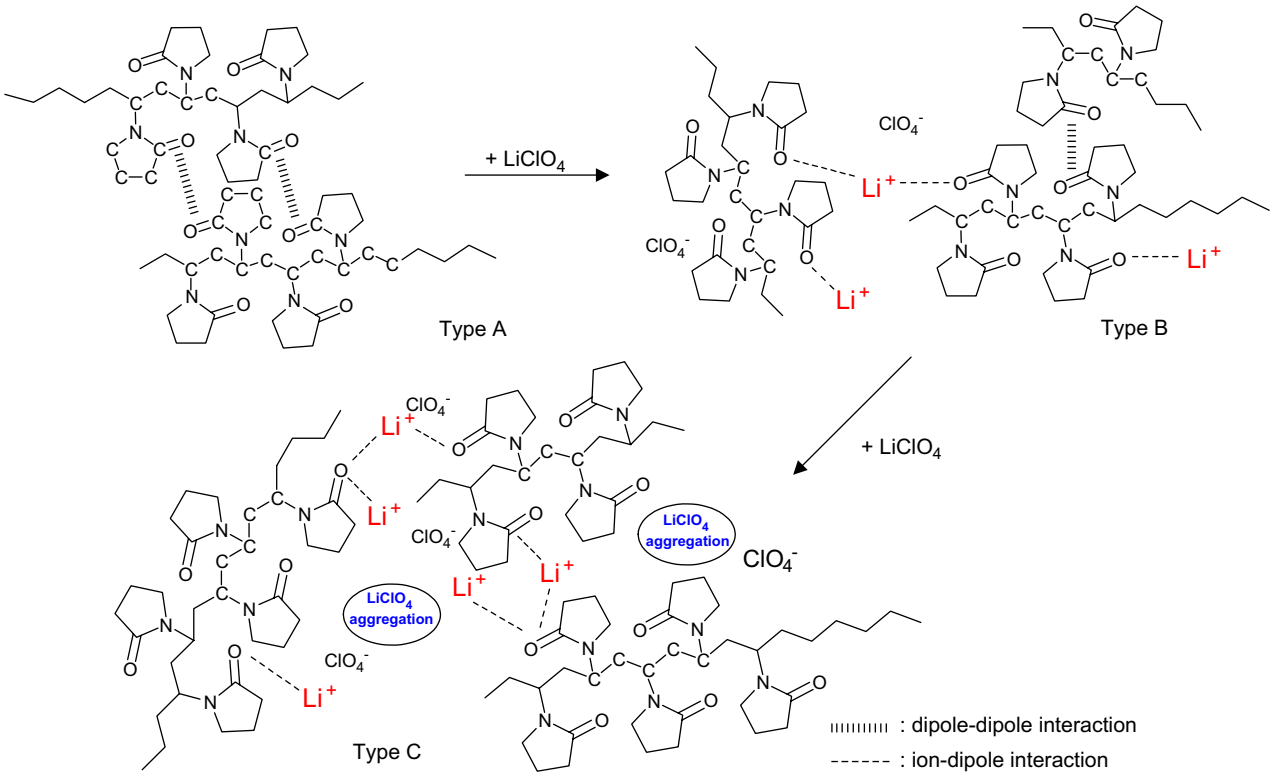

Fig. 8. Proposed association schemes for polymer electrolytes based on $LiClO_4$ and PVP.

To further clarify the complicated series of interactions that occur within these blended $LiClO_4$/PVP systems, in Fig. 8 we propose three modes of association. Type A describes the dipole–dipole interaction between the carbonyl groups of neat PVP. These interactions are disturbed or diminished when the ion–dipole interactions (type B) occur between the Li^+ ions and the carbonyl groups of PVP at a low $LiClO_4$ content. Type C indicates the situation that occurs when an excess of $LiClO_4$ causes the salt to aggregate.

Fig. 9 displays expanded FTIR spectra (from 1800 to 1650 cm^{-1}) recorded at 120 °C from a series of $LiClO_4$/

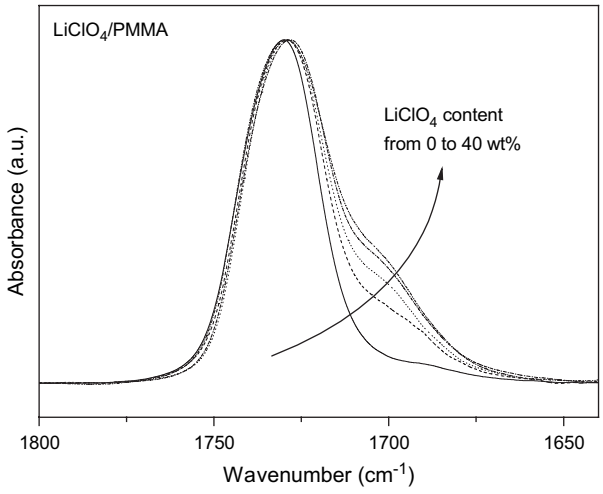

Fig. 9. IR spectra (C=O stretching region), recorded at 120 °C, of $LiClO_4$/PMMA blends containing varying $LiClO_4$ contents.

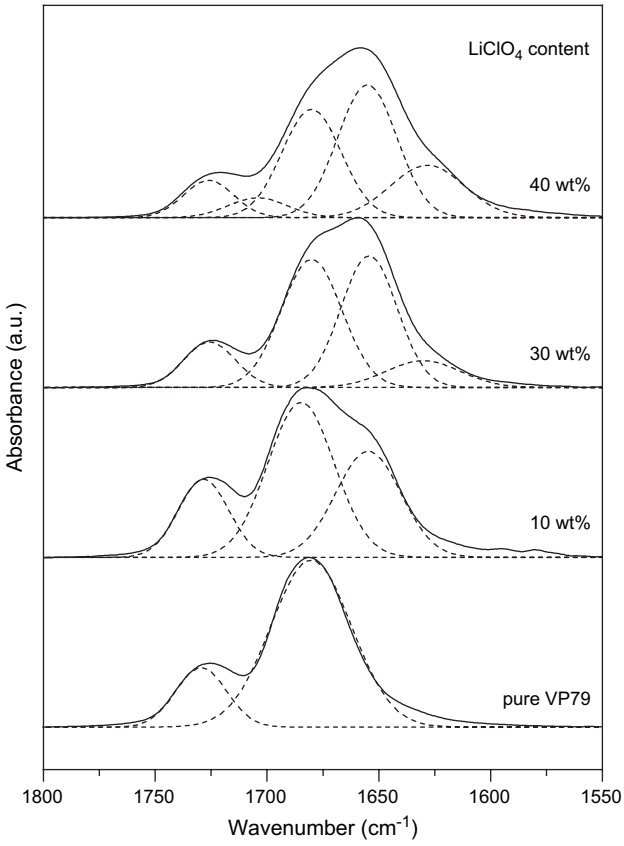

Fig. 10. Deconvolution of IR spectra (carbonyl stretching region: 1800–1525 cm^{-1}), recorded at 120 °C, of $LiClO_4$/VP79 blends containing various $LiClO_4$ contents.

PMMA blends. The stretching band of the free carbonyl group of the uncomplexed PMMA appears at 1730 cm^{-1}. When the $LiClO_4$ salt is added, a shoulder appears at ca. 1700 cm^{-1}, corresponding to C=O groups involved in ion–dipole interactions with Li^+ ions. It is clear in Fig. 9 that the relative intensity of this shoulder peak increases upon increasing the $LiClO_4$ concentration. Table 2 lists the results of curve fitting of the carbonyl group stretching bands of $LiClO_4$/PVP and $LiClO_4$/PMMA. The association between $LiClO_4$ and PVP is more preferable than that between $LiClO_4$ and PMMA. Furthermore, a band for a type-II complex, such as that which appeared in the spectra of the $LiClO_4$/PVP blend system at high $LiClO_4$ concentrations, was absent in the spectra of the $LiClO_4$/PMMA blends. We interpret these differences to the stronger dipole moments of the functional groups of PVP relative to those of PMMA. From a comparison with the DSC analyses, it appears that $LiClO_4$ tended to aggregate in the $LiClO_4$/PMMA blends at a lower salt concentration (ca. 30 wt%) than that found in the $LiClO_4$/PVP blends (ca. 50 wt%).

3.3. Blends of $LiClO_4$ and PVP-co-PMMA copolymers

Fig. 10 displays the results of deconvolution of the carbonyl stretching band region (1800–1525 cm^{-1}) of the IR spectra, recorded at 120 °C, of the $LiClO_4$/VP79 (i.e., PVP-*co*-PMMA containing 79 mol% of VP units) blend. We concentrated our attention on the unperturbed bands at 1680 and 1730 cm^{-1} for PVP and PMMA, respectively. As we mentioned above, the presence of a small amount of $LiClO_4$ (10 wt%) in PVP results in a new band at ca. 1654 cm^{-1}, which we assign to the signal of the "complexed I" C=O groups of PVP. When the $LiClO_4$ content is increased to 30 wt%, a band for the "complexed II" C=O groups of PVP appears at ca. 1630 cm^{-1}. Furthermore, a band appears for the "complexed" C=O groups of PMMA when the $LiClO_4$ content is further increased to 40 wt% (Fig. 9). Fig. 10 indicates that competition exists between the carbonyl groups of PVP and PMMA for their coordination to the Li^+ cations. At a low $LiClO_4$ content, Li^+ ions interact selectively with the PVP units only. When the $LiClO_4$ concentration is increased, the Li^+ ions begin to interact with both the PVP and PMMA units. Thus, it is clear that the Li^+ ions interact preferably with the PVP units over the PMMA ones. All of the carbonyl stretching signals of the $LiClO_4$/PVP-*co*-PMMA blends are clearly split into several bands that can be fitted well to Gaussian functions. For brevity, the results of the subsequent curve fitting are summarized in Table 3, which indicates that the relative intensity of the "uncomplexed" C=O groups of both the VP and MMA units decreases upon increasing the $LiClO_4$ content; a similar trend occurred for the individual $LiClO_4$/PVP and $LiClO_4$/PMMA binary blends. From a comparison between $LiClO_4$/PVP (30/70) and $LiClO_4$/VP57 (20/80)

Table 3
Curve-fitting results of IR spectra of C=O group stretching region recorded at 120 °C for the $LiClO_4$/PVP-*co*-PMMA blends with various $LiClO_4$ contents

Copolymers	$LiClO_4$ content, wt%	Carbonyl group in VP unit									Carbonyl group in MMA unit					
		"Uncomplexed" C=O			"Complexed I" C=O			"Complexed II" C=O			"Uncomplexed" C=O			"Complexed" C=O		
		ν, cm^{-1}	$w_{1/2}$, cm^{-1}	A_u, %	ν, cm^{-1}	$w_{1/2}$, cm^{-1}	A_{cI}, %	ν, cm^{-1}	$w_{1/2}$, cm^{-1}	A_{cII}, %	ν, cm^{-1}	$w_{1/2}$, cm^{-1}	A_u, %	ν, cm^{-1}	$w_{1/2}$, cm^{-1}	A_c, %
VP79	0	1682	35	100							1729	28	100			
	10	1684	34	60	1654	34	40				1728	27	100			
	20	1681	33	59	1654	33	41				1727	28	100			
	30	1681	32	43	1654	30	42	1630	39	12	1726	28	100			
	40	1681	31	34	1655	31	43	1628	39	23	1726	27	62	1704	31	38
VP57	0	1680	34	100							1729	28	100			
	10	1680	34	59	1655	32	41				1728	27	100			
	20	1680	33	46	1655	31	45	1629	38	9	1728	27	100			
	30	1680	32	35	1655	32	52	1629	40	13	1728	27	100			
	40	1681	32	29	1654	30	53	1627	40	18	1729	27	75	1705	30	25
VP47	0	1680	33	100							1729	28	100			
	10	1680	33	53	1655	32	42	1628	40	5	1728	27	100			
	20	1681	33	45	1654	32	45	1628	39	10	1729	27	81	1705	30	19
	30	1680	32	42	1654	31	45	1629	40	13	1730	28	75	1705	30	25
	40	1680	32	21	1655	30	61	1626	41	18	1728	27	58	1705	31	42
VP39	0	1680	33	100							1729	27	100			
	10	1680	32	59	1655	31	41				1729	27	100			
	20	1680	33	46	1655	31	47	1626	39	7	1730	28	75	1705	30	25
	30	1681	32	42	1654	30	46	1626	39	12	1730	27	72	1705	30	28
	40	1681	32	34	1654	30	44	1626	40	22	1730	27	61	1705	31	39
VP19	0	1680	33	100							1730	27	100			
	10	1680	32	41	1655	32	46	1628	40	13	1730	28	95	1705	30	5
	20	1680	32	32	1655	32	51	1628	40	17	1731	28	72	1705	30	28
	30	1681	32	9	1655	31	68	1627	39	23	1731	28	68	1706	31	32
	40				1655	30	74	1626	39	26	1729	27	66	1704	31	34

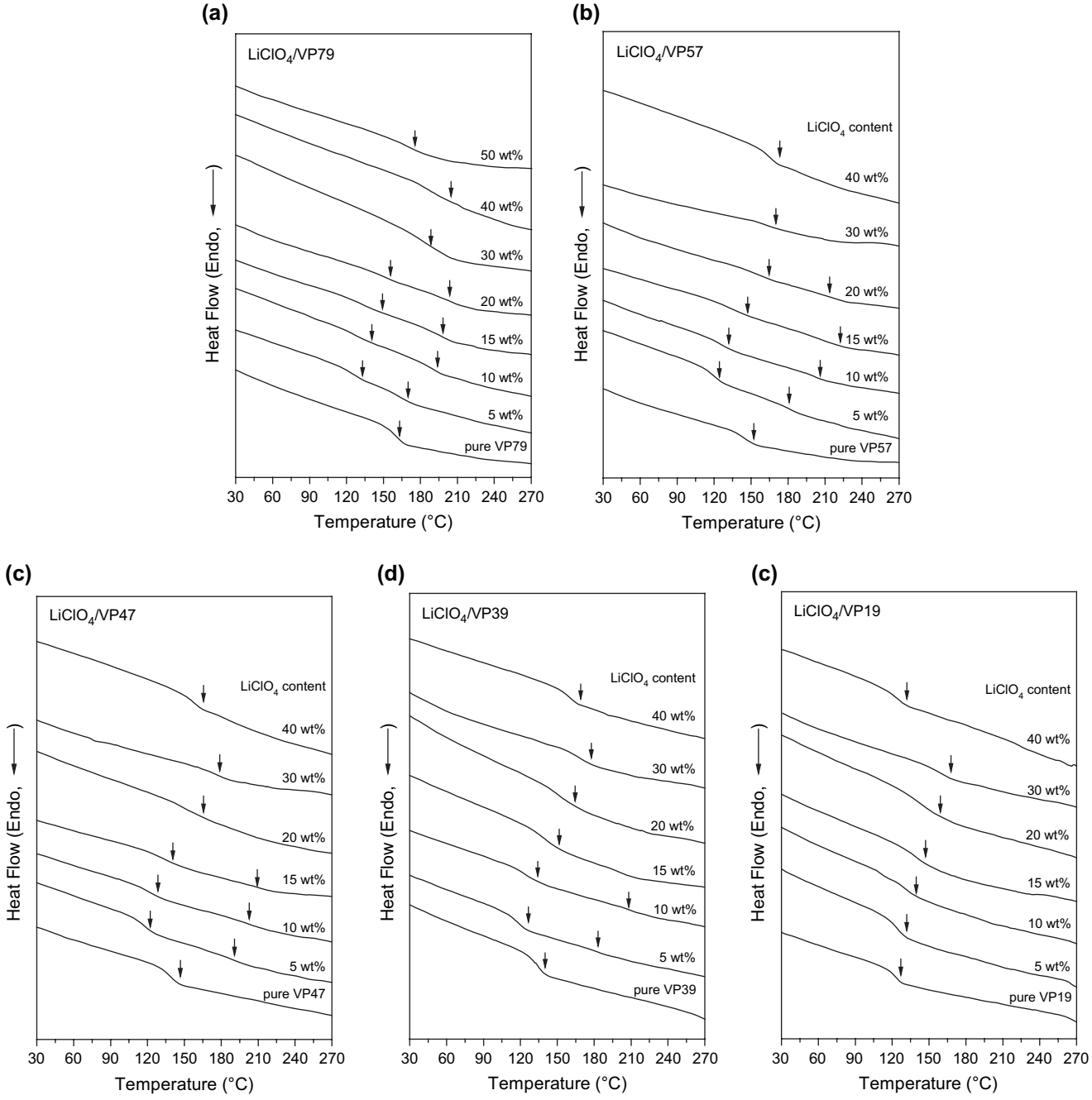

Fig. 11. DSC thermograms of $LiClO_4$/PVP-*co*-PMMA blends containing various $LiClO_4$ contents: (a) VP79, (b) VP57, (c) VP47, (d) VP39, and (e) VP19.

systems, both of which possess the same molar ratio of Li^+ ions to VP units, the area fraction of the ''uncomplexed'' C═O groups of the VP units in the latter blend system is lower than that of the former blend system. Because the MMA units in the PVP-*co*-PMMA copolymer play an inert diluent role to decrease the degree of self-association of the VP units, a lower $LiClO_4$ content is necessary for the $LiClO_4$/PVP-*co*-PMMA blend to attain the same degree of coordination between the Li^+ ions and the VP units.

DSC analysis is one of the most convenient methods for determining miscibility in polymer blends. In this study we measured values of T_g of our blends to identify their phase behavior. Fig. 11 displays the conventional second-run DSC thermograms that we obtained for various $LiClO_4$/PVP-*co*-PMMA blends; we identified either one or two glass transitions in each blend. The existence of a single glass transition strongly suggests that a blend is fully miscible and has a homogenous phase. In contrast, a blend containing two glass transitions is considered to be immiscible or phase separated. Fig. 12 presents the resulting phase diagram of the $LiClO_4$/PVP-*co*-PMMA blend at room temperature. Interestingly, even though each individual system—the PVP-*co*-PMMA copolymer and the $LiClO_4$/PVP and $LiClO_4$/PMMA blends—is miscible at all compositions, phase-separated loop exists

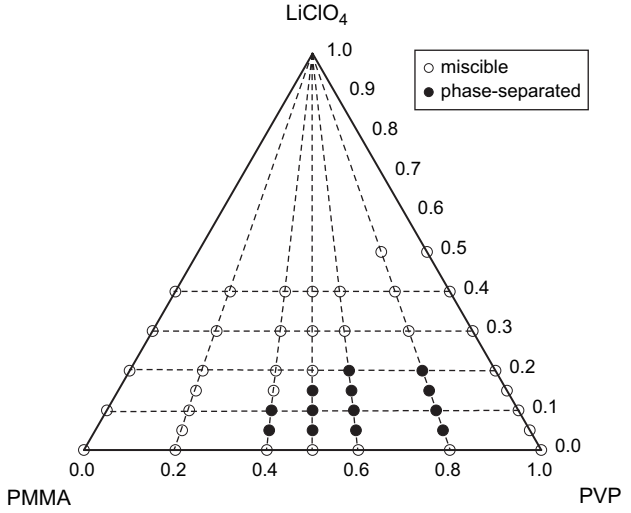

Fig. 12. Ternary phase diagram for the $LiClO_4$/PVP-*co*-PMMA system. Open circles represent miscible blends and full circles represent immiscible blends.

for certain compositions within the $LiClO_4$/PVP-*co*-PMMA blend system. The $\Delta\chi$ effect, i.e., the discrepancy between the interaction parameters χ of the third component with respect to polymers 1 and 2, plays an important role in dictating the phase behavior of these blends. The $\Delta\chi$ effect results from nonequivalent strengths of interaction between the different component pairs [41–43]. Zeman and Patterson [44] demonstrated that the $\Delta\chi$ effect strongly promoted the phase separation in ternary systems. Phase-separated loop occurs in systems that feature specific interactions when there is an ''attraction'' between the different covalently bonded monomers of the copolymers. From our FTIR spectroscopic analyses (Table 3), we found that $LiClO_4$ has a much greater preference for coordinating with PVP than with PMMA. Therefore, the addition of the third component, $LiClO_4$, tends to exclude the PMMA component in the $LiClO_4$/PVP-*co*-PMMA mixture such that it becomes immiscible. Moreover, the regions of phase-separated loop appear when the $LiClO_4$ content is low and/or the PVP component in the PVP-*co*-PMMA copolymer is relatively high. Nevertheless, when the $LiClO_4$ concentration is 30 wt%, the blends exhibit full miscibility regardless of the composition of the PVP-*co*-PMMA copolymer; enough $LiClO_4$ is available to interact with both the PVP and PMMA units simultaneously and, thus, the $LiClO_4$/PVP-*co*-PMMA blends become miscible. Fig. 12 indicates that a closed phase-separated loop exists in the phase diagram of the $LiClO_4$/PVP-*co*-PMMA blends as a result of the complicated set of interactions between the $LiClO_4$, PVP, and PMMA units.

Table 4 lists the values of T_g of $LiClO_4$/PVP-*co*-PMMA blends containing various $LiClO_4$ contents. The lower value of T_g, observed at ca. 123 °C, is close to that of neat PMMA and, therefore, it can be assigned to the glass transition of PMMA-rich domains. Likewise, we attribute the higher value of T_g (>180 °C) to the glass transition of the PVP-rich domains. Its presence implies that the PMMA phase is excluded from the mixture upon adding $LiClO_4$. In addition, the value of

Table 4
T_gs of $LiClO_4$/PVP-*co*-PMMA blends containing various $LiClO_4$ contents

PVP-*co*-PMMA copolymers	$LiClO_4$ content, wt%	T_g, °C
VP79	0	160
	5	126, 162
	10	126, 190
	15	133, 197
	20	154, 205
	30	189
	40	181
	50	167
VP57	0	144
	5	120, 182
	10	126, 202
	15	129, 208
	20	151, 198
	30	161
	40	166
VP47	0	139
	5	118, 194
	10	121, 204
	15	133, 209
	20	150
	30	179
	40	156
VP39	0	134
	5	119, 182
	10	123, 205
	15	137
	20	152
	30	169
	40	159
VP19	0	123
	5	125
	10	129
	15	139
	20	145
	30	159
	40	123

T_g of the PVP-rich domain in the $LiClO_4$/PVP-*co*-PMMA blend is higher than that observed for the binary blend of $LiClO_4$ and PVP containing the same $LiClO_4$ concentration. Because the presence of MMA moieties tends to reduce the degree of self-association of the PVP components, the Li^+ cations are better able to coordinate with the PVP units; this phenomenon results in the higher value of T_g. These results are consistent with those from our FTIR spectroscopic analyses. It is interesting that a random copolymer, PVP-*co*-PMMA, possessing covalently bonded monomers, undergoes phase separation upon doping the $LiClO_4$ salt at certain concentrations. Fig. 13 provides a schematic illustration of how we believe the phase separation process occurs in the $LiClO_4$/PVP-*co*-PMMA blends.

3.4. Ionic conductivity

Fig. 14 displays a plot of the room-temperature conductivity versus the VP content in the copolymer for $LiClO_4$/PVP-*co*-PMMA blends containing a fixed $LiClO_4$ content (20 wt%).

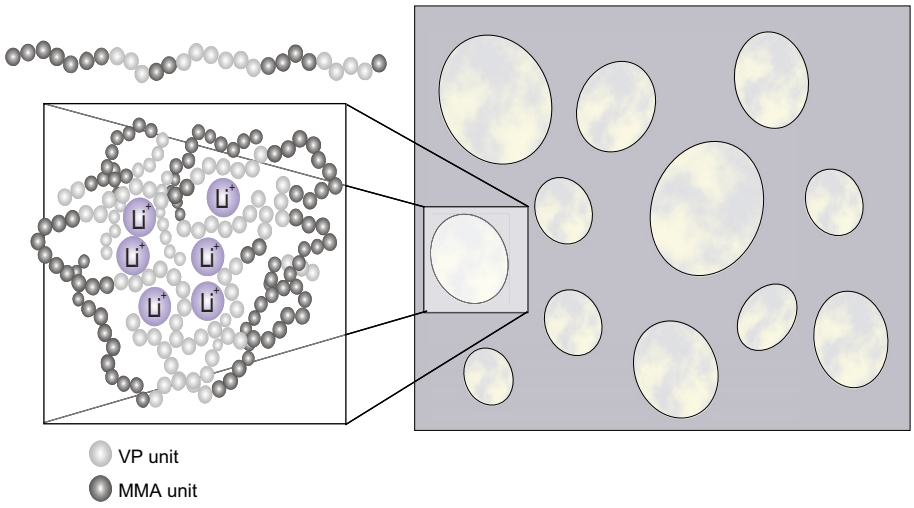

Fig. 13. Proposed schematic illustration of the phase separation occurring in $LiClO_4$/PVP-*co*-PMMA blends.

This plot indicates that the polymer electrolyte comprising $LiClO_4$ and VP39 exhibits the maximum ionic conductivity at room temperature. The conductivity (σ) behavior can be interpreted using the following equation [7,40,45]:

$$\sigma = \sum_i n_i z_i \mu_i \tag{4}$$

where n_i, z_i, and μ_i refer to the concentration of the charge carrier, the ionic charge on the charge carrier, and the mobility of the charge carrier, respectively. In this study, the ionic charge (z_i) is the same for all blend systems; thus, the resulting ionic conductivity depends only on n_i and μ_i.

We expected that the concentration of charge carriers (n_i) would be related to the fraction of "free" ClO_4^- anions that dissociated from the salt. Fig. 15 displays IR spectra, recorded at 120 °C, highlighting the region of the $\nu(ClO_4^-)$ internal vibration modes (660–600 cm^{-1}) for $LiClO_4$/PVP-*co*-PMMA blends containing a constant $LiClO_4$ content (20 wt%). Within this region, the absorptions at ca. 624 and 636 cm^{-1} correspond to the signals of the free anions and the contact ion pairs, respectively [46,47]. To clarify the charge environments of the ClO_4^- anions, we quantified the relative fractions of the free anion by decomposing the $\nu(ClO_4^-)$ internal vibration mode into two Gaussian peaks. Table 5 lists the relative fractional areas and the locations of the related adsorption bands. The relative fraction of the "free" ClO_4^- anions increased initially upon increasing the VP molar ratio of the PVP-*co*-PMMA copolymer, but it decreased when the VP molar ratio was over 60% (VP57). It is understandable that the incorporation of PVP moieties into PMMA tends to increase the relative fraction of the "free" ClO_4^- ions because the dipole moments of the pyrrolidone groups within the PVP molecules are strong enough to dissociate the $LiClO_4$ salt into its Li^+ and ClO_4^- ions. Shriver and Spindler [9] demonstrated, however, that the addition of Li^+, to form Li–PVP complexes, induces the N atoms within PVP to become quasi-cationic through electron resonance. These quasi-cationic N atoms of PVP attract

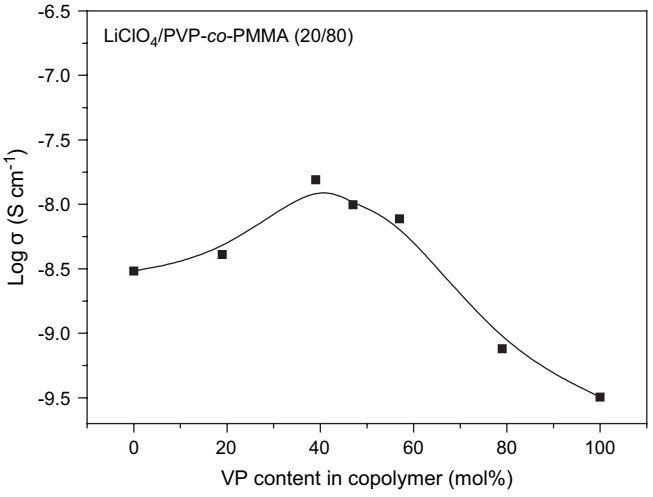

Fig. 14. Plots of the ionic conductivity at 30 °C of $LiClO_4$/PVP-*co*-PMMA blends versus the VP content of the PVP-*co*-PMMA copolymer.

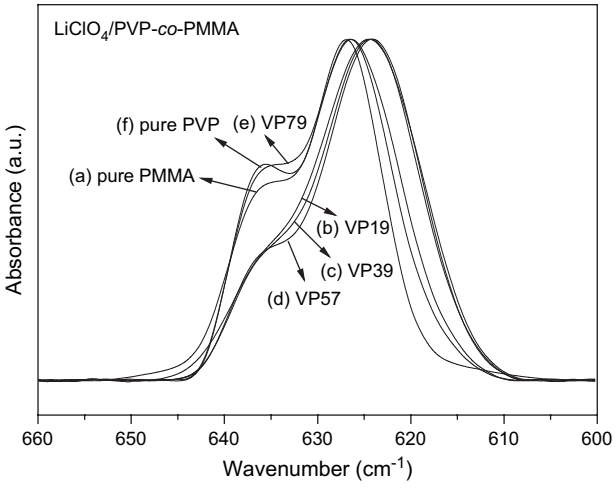

Fig. 15. IR spectra [$\nu(ClO_4^-)$ internal vibration modes] of $LiClO_4$/PVP-*co*-PMMA blends of various compositions.

Table 5
Curve-fitting data of infrared spectra at 120 °C of $\nu(ClO_4^-)$ internal vibration mode of $LiClO_4$/PVP-*co*-PMMA with various VP contents at a fixed $LiClO_4$ concentration = 20 wt%

Copolymers	Free anion			Contact ion pair		
	ν, cm^{-1}	$w_{1/2}$, cm^{-1}	A_f, %	ν, cm^{-1}	$w_{1/2}$, cm^{-1}	A_c, %
PMMA	626	10	76.3	637	6	23.7
VP19	625	11	80.8	636	7	19.2
VP39	624	11	84.7	636	7	15.3
VP47	624	10	84.7	636	6	15.3
VP57	624	10	84.9	636	6	15.1
VP79	626	10	79.8	637	6	20.2
PVP	625	10	71.1	636	6	28.9

the anions through coulombic interactions. Therefore, because the ClO_4^- anions can interact with both the Li^+ cations and the quasi-cationic N atoms of PVP, there is a decrease in the relative fraction of ''free'' anions.

On the other hand, it is reasonable to assume for solid-state electrolyte systems that the mobility of the charge carrier (μ_i) is related to the mobility of the polymer matrix (i.e., it depends on the value of T_g). For our system, however, the value of μ_i may be neglected because the values of T_g of the PVP-*co*-PMMA copolymers are all above room temperature. When considering the combination of effects that the values of n_i and μ_i have on the ionic conductivity, it is reasonable that the maximum ionic conductivity occurred for the $LiClO_4$/VP57 (20/80) system.

4. Conclusions

We have used DSC, FTIR spectroscopy, and ac impedance techniques to investigate in detail the miscibility behavior, interaction mechanisms, and ionic conductivities of polymer electrolytes comprising $LiClO_4$ and PVP-*co*-PMMA random copolymers. Although PVP/PMMA blends are immiscible [48], a single glass transition occurs for their corresponding copolymers, i.e., these copolymers are miscible. Furthermore, the MMA units in PVP play the role of an inert diluent that reduces the degree of self-association of the PVP units and, thus, causes negative deviation in the values of T_g. For the $LiClO_4$/PVP binary blend, we observed an unusual phenomenon: the addition of a small amount of $LiClO_4$ actually reduced the strength of the dipole–dipole interactions between PVP units and resulted in a decrease in the value of T_g. A subsequent increase in the $LiClO_4$ content led to an increase in the value of T_g of the PVP. It is interesting that the $LiClO_4$/PVP-*co*-PMMA polymer electrolyte exhibits an immiscibility loop in the phase diagram, even though each of its three individual systems—the PVP-*co*-PMMA copolymer and the $LiClO_4$/PVP and $LiClO_4$/PMMA blends—is miscible at every composition. Phase separation appears to occur through PMMA-rich domains being excluded from $LiClO_4$/PVP-*co*-PMMA blends. From a combination of the effects that the values of n_i and μ_i have on the ionic conductivity, the maximum conductivity occurred for the blend having the composition $LiClO_4$/VP57 (20/80).

Acknowledgments

This research was supported financially by the National Science Council, Taiwan, under Contract No. NSC-95-2216-E-009-001 and Ministry of Education ''Aim for the Top University'' program (MOEATU program).

References

[1] Armand MB, Chabagno JM, Duclot MJ. In: Vashishta P, Mundy JN, Shenoy GK, editors. Fast ion transport in solids. New York: North-Holland; 1979.
[2] Cheradame H, Le Nest JF. In: MacCallum JR, Vincent CA, editors. Polymer electrolyte reviews. New York: Elsevier; 1987/1989.
[3] Scrosati B. In: Scrosati B, editor. Applications of electroactive polymers. London: Chapman and Hall; 1993.
[4] Armand MB. Solid State Ionics 1983;9:745.
[5] Chao S, Wrighton MS. J Am Chem Soc 1987;109:2197.
[6] Bruce PG. Solid state electrochemistry. Cambridge: Cambridge University; 1995.
[7] Ratner MA, Shriver DF. Chem Rev 1988;88:109.
[8] Allcock HR, Ravikiran R, O'Connor SJM. Macromolecules 1997;30:3184.
[9] Spindler R, Shriver DF. Macromolecules 1986;19:347.
[10] Rajendran S, Uma T. Mater Lett 2000;44:242.
[11] Stephan AM, Kumar TP, Renganathan NG, Pitchumani S, Thirunakaran R, Muniyandi N. Solid State Ionics 2000;130:123.
[12] Appetecchi GB, Croce F, Scrosati B. Electrochim Acta 1995;40:991.
[13] Xu Y, Painter PC, Coleman MM. Polymer 1993;34:3010.
[14] Luo L, Ranger M, Lessard DG, Le Garrec D, Gori S, Leroux JC, et al. Macromolecules 2004;37:4008.
[15] Kennedy JP, Kelen T, Tüdös F. J Polym Sci Polym Chem Ed 1975;13:2277.
[16] Kelen T, Tüdös F. Macromol Sci Chem 1975;A9:1.
[17] Kuo SW, Chang FC. Polymer 2001;42:9843.
[18] Odian G. Principles of polymerization. New York: John Wiley & Sons; 1991 [chapter 6].
[19] Gordon M, Taylor JS. J Appl Chem 1952;2:493.
[20] Aubin M, Prud'Homme RE. Macromolecules 1988;21:2954.
[21] Kuo SW, Huang WJ, Huang CF, Chan SC, Chang FC. Macromolecules 2004;37:4164.
[22] Feldstein MM. Polymer 2001;42:7719.
[23] Painter PC, Graf JF, Coleman MM. Macromolecules 1991;24:5630.
[24] Kuo SW, Chang FC. Polymer 2003;44:3021.
[25] Xu H, Kuo SW, Lee JS, Chang FC. Macromolecules 2002;35:8788.
[26] Dong J, Fredericks PM, George GA. Polym Degrad Stab 1997;58:159.
[27] Chiu CY, Hsu WH, Yen YJ, Kuo SW, Chang FC. Macromolecules 2005;38:6640.
[28] Kuo SW, Wu CH, Chang FC. Macromolecules 2004;37:192.
[29] Eisenberg A, Rinaudo M. Polym Bull 1990;24:671.
[30] Chen HW, Chiu CY, Chang FC. J Polym Sci Polym Phys Ed 2002;40:1342.
[31] Kim JH, Min BR, Won J, Kang YS. J Phys Chem B 2003;107:5901.
[32] Chiu CY, Chen HW, Kuo SW, Huang CF, Chang FC. Macromolecules 2004;37:8424.
[33] Kim JH, Min BR, Kim CK, Won J, Kang YS. Macromolecules 2002;35:5250.
[34] Galin M. Makromol Chem Rapid Commun 1984;5:119.
[35] Martinez de Ilarduya A, Iruin JJ, Fernandez-Berridi MJ. Macromolecules 1995;28:3707.
[36] Moskala EJ, Varnell DF, Coleman MM. Polymer 1985;26:228.
[37] Zhu B, He Y, Yoshie N, Asakawa N, Inoue Y. Macromolecules 2004;37:3257.
[38] Hu Y, Motzer HR, Etxeberria AM, Fernandez-Berridi MJ, Iruin JJ, Painter PC, et al. Macromol Chem Phys 2000;201:705.

[39] Painter PC, Pehlert GJ, Hu Y, Coleman MM. Macromolecules 1999;32: 2055.
[40] Chen HW, Lin TP, Chang FC. Polymer 2002;43:5281.
[41] Zhang H, Bhagwagar DE, Graf JF, Painter PC, Coleman MM. Polymer 1994;35:5379.
[42] Ten Brinke G, Karasz FE, MacKnight WJ. Macromolecules 1983;16: 1827.
[43] Li XD, Goh SH. J Polym Sci Polym Phys Ed 2002;40:1125.
[44] Zeman L, Patterson D. Macromolecules 1972;5:513.
[45] Meyer WH. Adv Mater 1998;10:439.
[46] Mishra R, Rao KJ. Solid State Ionics 1998;106:113.
[47] Salomon M, Xu M, Eyring EM, Petrucci S. J Phys Chem 1994;98: 8234.
[48] Hsu WP. J Appl Polym Sci 2001;81:3190.